Characterizing the vulnerability of the national power grid of Sudan to space weather impact

Magdi Elfadil Yousif Suliman

Sudan University of Science and Technology, Physics Dept, Khartoum, Sudan

E mail magdi.yousif@sustech.edu, magdielfadil@gmail.com

Accepted: 14 September 2026

Abstract: Geomagnetic disturbances (GMDs) in geospace can significantly increase ground-based geomagnetically induced currents (GICs) through coupling processes. Therefore, the ground-space weather impact is mainly a high-latitude phenomenon. Nevertheless, this impact has been observed at mid- to low-latitudes. Notably, recurrent blackouts occurred in the National Power Grid of Sudan (NPGS), and the grid has recently undergone expansion. Aiming to identify NPGS's potential vulnerability to space-weather impact and infer causality logic, we've developed an indirect exploration method. Two categories of blackout events were differentiated: those synchronous with GMDs, i.e., a storm or sudden commencement, SI (the Blackout-GMDs events), and those asynchronous with either. However, storms are classified according to class, type, or phase. Class includes severe, major, and minor; type is either driven by a co-rotating interaction region (CIR) or driven by coronal mass ejections (CME); phases are initial, main, or recovery. The Blackout-GMDs events are investigated for their relation with yearly mean total sunspot numbers. According to the NPGS location, inferring the space-weather impact is attributed to the spectral content of the GMDs, we have investigated whether Blackout-GMDs events are associated with ground-simultaneously observable mid- to low-latitude Pc5 geomagnetic pulsations. Results have shown that 49% of blackout events are Blackout-GMDs events. The 4th-degree polynomial fits for the number of occurrences of Blackout-GMDs events, and the yearly mean total sunspot numbers are remarkably correlated. All Blackout-GMDs events are associated with globally simultaneously-observed mid- to low-latitude Pc5 pulsations. This suggests that the NPGS is most likely vulnerable to space weather impact.

Key words: Space weather impact; mid- to low-latitudes; blackouts in power grids; Pc5 geomagnetic pulsations

1. Introduction

Space weather ground impact in high-latitude locations was recognized long ago, over about 150 years ago (e.g., (Kelbert 2019) and the references therein). The ground impact is manifested as electromagnetic interactions with ground conducting systems, including early telegraph systems, pipeline networks, railway networks, and power grid systems. As a result of affection by such an impact, these systems might encounter multiple problems, for instance, malfunctions or severe cases of damage. The geomagnetic disturbances (GMDs) play viable role in the electromagnetic coupling that leads to this impact. Those problems result because some components of such systems, particularly in severe cases, sustain partial damage, experience operational disruptions, or undergo system malfunctions. Regarding power grids, the worst-case scenario expected to present from such an impact is damage to components in parts of the grid, resulting in malfunctions that cause blackouts. The space weather ground impact has been evidenced originally to occur in high-latitudes ground locations, for instance, in Canada and Nordic countries (e.g., (Boteler 2001; 2019), (Boteler D. H. et al. 1998) and (Heikki Nevanlinna et al. 2001; Pirjola 2005)).

However, the impact of space weather on conducting systems in high-latitude locations depends on the severity or amplitude content of GMDs, since the direct electromagnetic coupling associated with GMDs enhances geomagnetically induced currents (GICs) in the ground at these locations. Where, at these locations, auroral electrojet current systems driven by the GMDs give rise to problems in power grids. A key step towards a theoretical approach to evaluating the contributions of the auroral electrojet current systems to enhance GICs is to calculate the electric and magnetic fields necessary for identifying the GICs at high-latitude electromagnetic phenomena (Boteler D. H. & J. 1998). On the other hand, at mid- to low-latitude locations, space weather impacts on power grid systems have been observed, even though the average amplitudes of GICs are smaller than those at high latitudes. However, power grids at mid- to low-latitude are still vulnerable to the impact of space weather, since GICs also depend on other conditions, e.g., Earth's conductivity, the grid parameters, and spectral content within the GMDs. Spectral content here refers to the constituent frequencies or time scales of complex magnetic field fluctuations associated with the GMDs. Therefore, considering the cause-and-effect linking of the phenomenon of the impact of space weather at mid- to low-latitude locations, former researchers have reported in their previous work that this impact could be observed on the ground at mid- to low-latitude locations, e.g., (Jacko Koen & Gaunt 2003; Liu et al. 2009; Ngwira et al. 2011; Trivedi et al. 2007; Watari S. et al. 2009).

Geomagnetic disturbances with spectral content mostly account for the possibility of observing the impact of space weather at unexpected mid- to low-

DOI: 10.31401/SunGeo.2026.01.02

latitude locations on the ground. These disturbances contain complexity fluctuations in the associated magnetic field, which may contribute to producing sufficiently intense geoelectric fields, because their accompanying spectral component can stimulate a ground response that enhances sufficient GICs and affects the conducting systems at these locations. However, GMDs with favorable spectral content are observed when mechanisms of geomagnetic pulsations and their sources are upstream of the solar wind within the interplanetary shock region, or their associated geomagnetic pulsations are observed on the ground at mid- to low-latitude locations. Since mid- to low-latitude Pc5 geomagnetic pulsations correlate with solar wind, we envisage that these Pc5 pulsations play a key role in interpreting space weather phenomena at those locations. In a former study the spectral content has been proposed to act equally important as the GMDs amplitude in producing the space weather impact at these locations, e.g., (Kappenman 2003) has shown that regardless of conditions on the ground as long as the high spectral content of the incident magnetic field disturbance of the GMDs, the higher will be the relative geoelectric field response. The geoelectric field is an essential variable used in calculations to obtain GICs via a specific formula (Ngwira et al. 2011). Nevertheless, other parameters specify the GICs' effect on power grids at mid- to low-latitude ground locations, for instance, the grid parameters including: the network topology, station coordinates, transformer resistances, transmission line resistances, and station earthing resistances, and the ground conductivity (e.g., (Zhang et al. 2015) and the references therein). Worth noting that observations of the space weather impact on power grid systems located in mid- to low-latitude ground locations are yet to be extensively undertaken; for instance, to the best of our knowledge, the National Power Grid of Sudan (NPGS) has never before been examined for its vulnerability to space weather impact. Moreover, Sudan is hardly able to sustain stability in power production. However, in the country, there are multiple sources of energy production, such as hydroelectric power plants, that is, dams in the Nile, thermal power plants, and other renewable sources of power, so addressing the topic of the possibility of vulnerability of Sudan's grid to space weather impact is vital, focusing on outlining challenges to guarantee power production stability in the near future. In this study, we have presented a characterization of blackout events, that is, the records of blackout events that occurred in the NPGS, which might be attributed to potential GMDs, exemplifying the vulnerability of the NPGS to the impact of space weather.

2. Data and analyses

In this work, the focus was on studying recurrent blackouts in a power grid located in a mid- to low-latitude region. The question is how to characterize these blackouts in terms of what possible natural cause, specifically to assess whether some of them are associated with GMDs (the Blackout-GMDs events). With respect to the Blackout-GMDs events, we have examined whether these disturbances exhibit features that demonstrate their capability to produce space weather impacts on power grids in mid- to low-latitude regions. Dates of blackouts (DDMMYYYY) in the National Power Grid of Sudan (NPGS) were collected and termed blackout events. The blackout events data have been provided to us courtesy of the Sudanese Electricity Transmission Company Ltd. Information about the grid and a map are available on the website of the Global Energy Network Institute (GENI) (Global Energy Network Institute 2017), see the map of the grid in Fig. 1. However, a period was chosen within which the collected data were available. The period roughly included the descending phase of solar cycle 23 and the ascending phase of solar cycle 24. That is, the period was from 2001 to 2013. Within this period, quite a noticeable number of blackout events were recorded. There were 37 blackout events. The occurrence of these blackout events is shown in the upper panel of Fig. 2, and the lower panel shows yearly mean total sunspot numbers for the same time span, shown also are the 4th degree polynomial fitting plots.

2.1. GMDs data sets

The geomagnetic disturbances (GMDs) considered on the analysis include storms and interplanetary shock sudden impulse (SI). And, in order to investigate the onset of either a geomagnetic storm or an interplanetary shock impulse (SI), we looked at their well-known features appearance on the disturbance in the storm time index ("Dst"), actually with respect to storms we looked at the minimum "Dst". The time series data of the storm time index, i.e., the final Dst Data, were collected from the World Data Center for Geomagnetism of Kyoto (Nose et al. 2015). Furthermore, to categorize geomagnetic storms by their potential solar wind-based drivers, a set of time series plots of solar wind parameters data was collected. The parameters include Solar wind proton number density ("n"), solar wind bulk speed ("Vsw"), and solar wind radial components of the proton temperature ("T"). In addition to those solar wind parameters, the set also includes time series data of interplanetary magnetic field ("MFI") components, that is, it includes: the magnitude ("MFI ⟨|B|⟩"), and the three vector components in GSE Cartesian coordinates ("MFI Bx", "MFI By" and "MFI Bz"). All the aforementioned set of geospace and magnetospheric data were obtained from ACE satellites missions, the data are well organized and arranged in the website of the Coordinated Data Analysis Web (CDAWeb), and made available from two sources: the source of the solar wind parameters (Smith & Ness 2022) and the source of the Interplanetary magnetic field components (McComas et al. 2022).

2.2. Geomagnetic data sets

Geomagnetic data from a set of selected ground stations were obtained, and we analyzed the persistence of continuous pulsations (Pc5 pulsations) occurring within times of the Blackout-GMDs events.

These pulsations have been extracted from magnetic field data from the stations that are located in locations around the globe to cover different local times (LTs). The stations belong to the International Real-time Magnetic Observatory Network (INTERMAGNET) chain of magnetometers. The stations and their related necessary information are listed in Table 1.

Table 1. Details of INTERMAGNET stations, of which the data are used

The INTERMAGNET station name	Station code	Geodetic coordinates (Latitude, Longitude)	*L- Shell value
Honolulu	HON	21.3200N, 158.0000W	0.975563
San Juan	SJG	18.1100N, 66.1500W	1.01537
Guimar	GUI	28.3210N, 16.4410W	1.27921
Tamanrasset	TAM	22.7900N, 5.5300E	1.22582
Kanoya	KNY	31.4200N, 130.8800E	1.07624

* The L-Shell value calculator in the website, cited as: (GeoMagSphere 2025) is used.

2.3. The analyses

Since, there are significant number of blackouts within the selected span, total of 37 blackout events, a preliminary check with yearly mean total sunspot numbers has shown that there is obvious correlation between the 4th degree polynomial fit for blackout events number occurrence and yearly mean total sunspot numbers data, Fig. 2. Therefore, and motivated by this result, other steps of the analyses were followed. First, exploring whether any of the blackout dates is either synchronous or asynchronous with GMDs, a storm or SI, that is for each blackout date in the records within the span, that was done such that the date of the blackout was taken for reference for the onset of either of these GMDs. The "Dst" index data were used to identify types of the geospace perturbations, i.e., a storm (all classes), or SI. The classes of storms were illustrated as follows: severe ("Dst ≤ -150 nT"), major ("-50 nT ≥ Dst > -150 nT"), and minor ("Dst > -50 nT"). And, the geomagnetic storms were categorized into types, based on the possible driver, i.e., whether a Coronal Mass Ejection (CMEs) or a Co-rotating Interaction Region (CIR), differences between CME and CIR driven storms are summarized in (Borovsky & Denton 2006). To examine each type of storm according to the driver, the plotted graphs of time series data of solar wind parameters and the interplanetary magnetic field components data were utilized. Second, considering only the Blackout-GMDs events, regardless of the magnetosphere disturbance driver, and inferring the spectral content of the GMDs leads to the space weather impact represented in the occurrence of the blackout events, since the ground location is a mid-low latitudes, therefore an analysis was carried out in order to characterize whether Blackout-GMDs events is also associated with a low-latitude Pc5 geomagnetic pulsation amplitudes' enhancements (Sakharov et al. 2022). The Pc5 pulsations were obtained from the geomagnetic data of ground low-latitude stations belong to the INTERMAGNET network, that were carefully selected, so that a simultaneous global appearance of the Pc 5 pulsations with similar enhancement feature can be investigated.

3. Results and discussion

The total blackout events in the NPGS, the 37 events, were characterized in terms of Blackout-GMDs events, for storms all types and classes, and blackout events asynchronous GMDs, the pie chart in Figure 3 shows results. Interestingly, the chart shows that 49% of the total blackout events were Blackout-GMDs events. The Blackout-GMDs events are further characterized in terms of the GMDs, whether a storm (all types, classes, and phases), or sudden shock impulse. Worth noting that the power generation system in the NPGS includes various types of generating units of thermal generation and hydro generation that complement the grid. Also, it is witnessed that recently the grid has been developed largely based on hydroelectric power, by linking some tens of megawatts of hydroelectric power stations with the main load in the capital, Khartoum. Such specifications of the NPGS emphasize the scale of extension in the grid and the density of interconnections, both can justify the vulnerability of the grid to space weather impacts.

3.1. Highlighting features of GMDs, for blackout events synchronous GMDs

Results of characterizing blackout events showed that 16 blackout events are Blackout-GMDs events. So, to clarify specifications of these storms, classes of these storms were identified according to the minimum Dst, whether severe, major, or minor. Moreover, the storm's possible drivers have been identified, whether Coronal Mass Ejections (CMEs) or Co-rotating Interaction Regions (CIRs). The adopted method is to investigate certain features on the interplanetary magnetic field and the solar wind parameters of the plotted graphs of the simultaneous time series data, i.e. for interplanetary magnetic field: the total field, x, y, and z components of the field in GSE coordinates, and the solar wind parameters: density, speed, and temperature. The storm is identified as a CME-driven storm if peaks are simultaneously observed in the aforementioned parameters of interplanetary magnetic field and the solar wind. According to CME driven storms morphology and parameters differentiating between them and CIR driven storms (Borovsky & Denton 2006), the associative interplanetary shock is interpreted as appearance of simultaneous peaks on the parameters, including the solar wind: speed, density, and temperature, and the interplanetary magnetic field: x, y, and z components, and total field. On the other hand, the storm is identified as a CIR-driven storm if peaks are simultaneously observed on the parameters of the interplanetary magnetic field and the solar wind, except that the solar wind speed must pass through an abrupt transition from low to high speeds. Correspondingly, there are fluctuations on the z-component of the interplanetary magnetic field, changing its direction from northward to southward. Results of these analyses for the rest of the blackout events are summarized in Table 2.

Table 2. Blackout events synchronizing each class and type of storm (According to the minimum Dst and the driver) or interplanetary shock, SI, or asynchronous with either

Storm class	Storm Phase	Minimum Dst	A storm Type (Driver)	Date of blackout event day/ DDMMYYYY SG: Graded storm (No obvious preliminary shock).
Minor	Recovery	-36, -46, -35	CIR; CIR; CIR	10062001; 07082005; 24012010
	Main	-42	CME	04022009
	Initial	-40	CIR	03052006
Major	Recovery	-85, -106, -106, -139, -59	CME; CIR; CIR; CME; CIR	19102003 (SG); 14062005 (SG); 19062005; 16092005; 17022010 (SG)
	Main	-64, -57, -81	CME; CIR; CME	09102001 (*SG); 19102001 (SG); 06042010 (SG)
	Initial	-56	CME	12122004
Sever	Recovery	-166, -292	CME; CIR	07102001; 08112001
	Main	Non	Non	
	Initial	Non	Non	
Sudden impulse shock (SI)	09012003; 12012008			
Blackout events asynchronous storm or sudden impulse, SI	04082001; 06122001; 21072002; 16082003; 11102003; 25072005; 17012007; 12062008; 20122008; 11072009; 04102009; 26112009; 30112009; 12012010; 15032010; 04112010; 28082011; 18122013; 21122013			

The table showed blackout events synchronous with storm time according to storm class, and type (due to storm possible driver). Characterizing only the Blackout-GMDs events, for storms (all classes and types), and the results are in Fig. 4. Interestingly, results have shown that the greatest number of blackouts events occurred in the recovery phase for all class and types of storms compared with the two other phases of storms: 28% (Recovery), 17% (main) and 5% (initial), 17% (Recovery), 6%(main) and 5% (initial), and 11% (Recovery), 0%(main) and 0% (initial) for major, minor and severe storms, respectively.

3.2. Pc5 pulsations relation with the blackout events synchronous GMDs

Space weather impact at the ground mid–low latitudes locations basically is attributed to spectral content of the geomagnetic disturbances, GMDs. Noting that geomagnetic pulsations in the Pc5 range have been identified for a global appearance commonly during geomagnetic storms, and also have been globally initiated during sudden impulses, e.g., (Marin et al. 2014; Samsonov et al. 2011). Therefore, the activity of global appearance, in mid-low latitude ground geomagnetic stations, of Pc5 pulsations have been investigated, whether related to either of the Blackout-GMDs events. The magnetograms include filtered geomagnetic data (150 – 600 s) and spectrograms, i.e., three components of the geomagnetic field. The geomagnetic data used in obtaining these magnetograms spanned to cover the day of the Blackout-GMDs events, that is 72 hours before and 72 hours after the blackout day (168 hours centered at the day (24 hours) when the Blackout-GMDs events have occurred). These magnetograms are obtained for geomagnetic data from all stations listed in Table 1, and they are stacked to observe features on Pc5 pulsation activity in enhancement of amplitudes. Even though these stations are distributed in widely separated longitudinal manner, the results have shown that there is an outstanding amplitudes similar enhancement features in almost all stations observing the Pc5 pulsations that associated with all blackout events synchronous storms or sudden impulse shock. The limitations exist just because of the data discontinuity and gaps in some stations. Presented here are just samples of magnetograms from data of stations giving examples of the results. Shown here are examples for each individual GMDs, covering all storms (different classes) showing association of mid-low latitude Pc5 pulsations amplitude simultaneous enhancements features to blackout events synchronous storms or SI. Fig. 5 depicts magnetograms for Pc5 pulsations amplitudes that obtained from four stations, details of which are previously shown in Table 1. The magnetograms data are centered at the day the blackout event (08112001) occurred synchronous with a severe storm. With respect to blackout events synchronous major and minor storms Fig. 6, and Fig. 7, show magnetograms for Pc5 pulsations amplitudes that obtained from four INTERMAGNET stations earlier mentioned here, the magnetograms data are centered at the days of the blackout events (12122004) and (04022009) occurred synchronous with major and minor storms, respectively. The final example of results shown in Fig. 8 depicts magnetograms for Pc5 pulsations amplitudes obtained from four INTERMAGNET stations, The magnetograms data are centered at the day the blackout event (12012008) occurred synchronous with an interplanetary magnetospheric shock sudden impulse, SI. In all these magnetograms Pc5 pulsations amplitudes enhancements feature is shown with the oval shape, the enhancement feature is obvious for the horizontal components of the geomagnetic field, implies compressional source in the geospace. The Pc5 amplitudes enhancement feature occurred some hours before the blackout event in the case of severe storms, simultaneously synchronous with the blackout event day in the case of major minor, and SI, but also extended post the blackout event day in the case of SI.

3.3. Discussion

The blackout events number occurrence within the selected time span period are quite remarkable and the Blackout-GMDs events almost half of them (49 %). The time span of the collected blackout events data in the NPGS is roughly covered the descending phase of the solar cycle 23 and the ascending phase of solar cycle 24, intentionally supporting to investigate blackout events occurrence relation to the cyclic variations on conditions controlling space weather and consequently its impact at a low-latitude ground location. An outstanding 4th degree polynomial fit relationship is found between the blackout events number occurrence and the yearly mean total sunspot numbers reveals that the space weather impact is crucial for the NPGS, power grid, laid at ground mid-low latitude region. These results suggest contribution of geospace disturbances, GMDs in blackout events in the grid, but other important features on the GMDs to indicate impact on ground systems, as on grids, at mid-low latitudes are the associative spectral contents of these GMDs. Ground mid-low latitude Pc5 pulsations customarily are related directly to originate on solar wind, e.g. pressure, or streams at the bow shock. That is during geomagnetic activity the magnetosphere region becomes source of Ultra Low Frequency (ULF) hydrodynamic waves. And the signature of these ULF waves in the ground magnetic field is what is known as geomagnetic pulsations, whence Pc5 is just a period or frequency range (1.67-6.67 mHz). These Pc5 pulsations might have global wide appearance in the ground. It has been also known that the spectral content of these pulsations causes enhancements on the geomagnetically induced currents, GICs, on the ground at mid-low latitudes, and consequently may contribute on causing blackout in such latitudes. The features on the GMDs relate them to the blackout events in the case of the NPGS are suggested to be traced by the mid-low latitude Pc5 pulsations activity as indicators for the relationship between blackout events and GMDs. In Fig. 5 shows the blackout event (08112001) that synchronous a severe storm and a simultaneous global appearance of enhancements on amplitudes of Pc5 pulsations occurred at four mid-low latitude stations quite separated longitudinally, the enhancements started about 24 hours before the day of the blackout event occurrence. In Fig. 6, Fig. 7, and Fig. 8 show blackout events, (12122004), (04022009), and (12012008) that synchronous major, minor, and sudden impulse , SI, respectively. In all these events a simultaneous global appearance of enhancements on amplitudes of Pc5 pulsations occurred at four mid-low stations, on the same day of the blackout events for the events synchronous major and minor storms and on the same and post the day of blackout event synchronous the sudden impulse. However, the rest of all the blackout events synchronous a GMDs, i.e. the

14 blackout events synchronous a GMDs, not shown here, are all associated with similar simultaneous global appearance of enhancements on amplitudes of mid-low latitude Pc5 pulsations. This exploration demonstrates the importance of the spectral content of the Pc5 pulsations as a mechanism leads to space weather impact at mid-low latitude locations regardless of the type of the GMDs whether a storm or a sudden impulse, SI.

4. Conclusion

We conclude that the blackout events in the NPGS, which are synchronous to GMDs, are correlated to seasonal cycle variations in the solar conditions that control space weather, i.e., to the yearly mean total sunspot numbers. And this indicates that these blackout events are related to a space-weather-origin-driven mechanism. This final analysis is supported by the associative appearance of a mid- to low-latitude Pc5 pulsation globally occurring within a period centered at the day of the blackout event occurrence. Also, the final analysis is that the significant space-weather-impacted mid- to low-latitude locations were during minimum solar-weather drivers, i.e., low sunspot numbers, and during the recovery phase of geomagnetic storms. Therefore, the continuous observations of mid- to low-latitude Pc5 pulsations are vital for the investigation of space-weather impact in mid- to low-latitude ground locations.

5. Recommendations

In future work, we will consider carrying out regression analyses by taking multiple parameters, including solar wind parameters, i.e., solar wind speed, pressure, proton density, and temperature, in addition to mid-low latitude geomagnetically induced current amplitudes. The analysis may help in identifying the extent to which the former parameters determine GICs in mid-low latitude ground locations. Ultimately, we would like to point out for necessity of upholding campaigns of installations of space weather ground data instruments in particularly in mid-low latitude locations on the globe, in exceptionally challenging regions, just like Sudan.

6. Acknowledgement

The results presented in this paper rely on data collected at magnetic observatories. We thank the national institutes that support them and INTERMAGNET for promoting high standards of magnetic observatory practice (www.intermagnet.org). Also, we thank engineer, Haitham Ahmed Mohamed Hashim, Operation Manager, national load dispatch center, Sudanese Electricity Transmission Company Ltd. (SETCO) for his kind help and support by providing us with the blackout events data, a copy of the original data sheet contains the data is available on demand.

References

Borovsky, E. J. & Denton, H. M. 2006, Journal of Geophysical Research 111, 7.
Boteler D. H. & J., P. R. 1998, Geophysics Journal International 132, 31.
Boteler D. H., Pijola R. J. & H, N. 1998, Advances in Space Research 22, 17.
Boteler, D. H. 2001, Space Weather Geophysical Monograph 125.
Boteler, D. H. 2019, Space Weather 17, 1427.
GeoMagSphere 2025, vol. 2025.
Global Energy Network Institute 2017 (San Diego, California 92138, USA: R. Buckminster Fuller Centennial Celebration, San Diego, California), vol. 2026.
Heikki Nevanlinna, Pentti Tenhunen, Risto Pirjola, Jaakko Annanpalo & Pulkkinen, A. 2001, Journal of Atmospheric and Solar-Terrestrial Physics 63, 1099.
Jacko Koen & Gaunt, T. 2003, 2003 IEEE Bologna PowerTech Conference (Bologna, Italy: IEEE).
Kappenman, J. G. 2003, Space Weather 1.
Kelbert, A. 2019, Surveys in Geophysics 41, 115.
Liu, C.-M., Liu, L.-G. & Pirjola, R. 2009, IEEE Transactions on Power Delivery 24, 2368.
Marin, J., Pilipenko, V., Kozyreva, O., Stepanova, M., Engebretson, M., Vega, P. & Zesta, E. 2014, Annales Geophysicae 32, 319.
McComas, D., Skoug, R., Delapp, D., Elliott, H. & Davis, A. 2022, ACE Solar Wind Electron Proton Alpha Monitor (SWEPAM) 64-Second Level 2 Data (NASA Space Physics Data Facility 0% Journal Article).
Ngwira, C. M., McKinnell, L.-A. & Cilliers, P. J. 2011, Advances in Space Research 48, 529.
Nose, M., Iyemori, T., Sugiura, M. & Kamei, T. 2015, Geomagnetic Dst index.
Pirjola, R. 2005, Advances in Space Research 36, 2231.
Sakharov, Y. A., Yagova, N. V., Pilipenko, V. A. & Selivanov, V. N. 2022, Russian Journal of Earth Sciences 22, 1.
Samsonov, A. A., Sibeck, D. G., Zolotova, N. V., Biernat, H. K., Chen, S. H., Rastaetter, L., Singer, H. J. & Baumjohann, W. 2011, Journal of Geophysical Research: Space Physics 116, n/a.
Smith, C. W. & Ness, N. F. 2022, ACE Magnetic Field (MAG) Geocentric Solar Ecliptic, GSE, and Geocentric Solar Magnetospheric, GSM, Coordinates, Level 2 (H1), 4 min Data (NASA Space Physics Data Facility 0% Journal Article).
Trivedi, N. B., Vitorello, Í., Kabata, W., Dutra, S. L. G., Padilha, A. L., Bologna, M. S., de Pádua, M. B., Soares, A. P., et al. 2007, Space Weather 5.
Watari S., Kunitake M., Kitamura K., Hori T., Kikuchi T., Shiokawa K., Nishitani N., Kataoka R., et al. 2009, Space Weather 7.
Zhang, J. J., Wang, C., Sun, T. R., Liu, C. M. & Wang, K. R. 2015, Space Weather 13, 643.

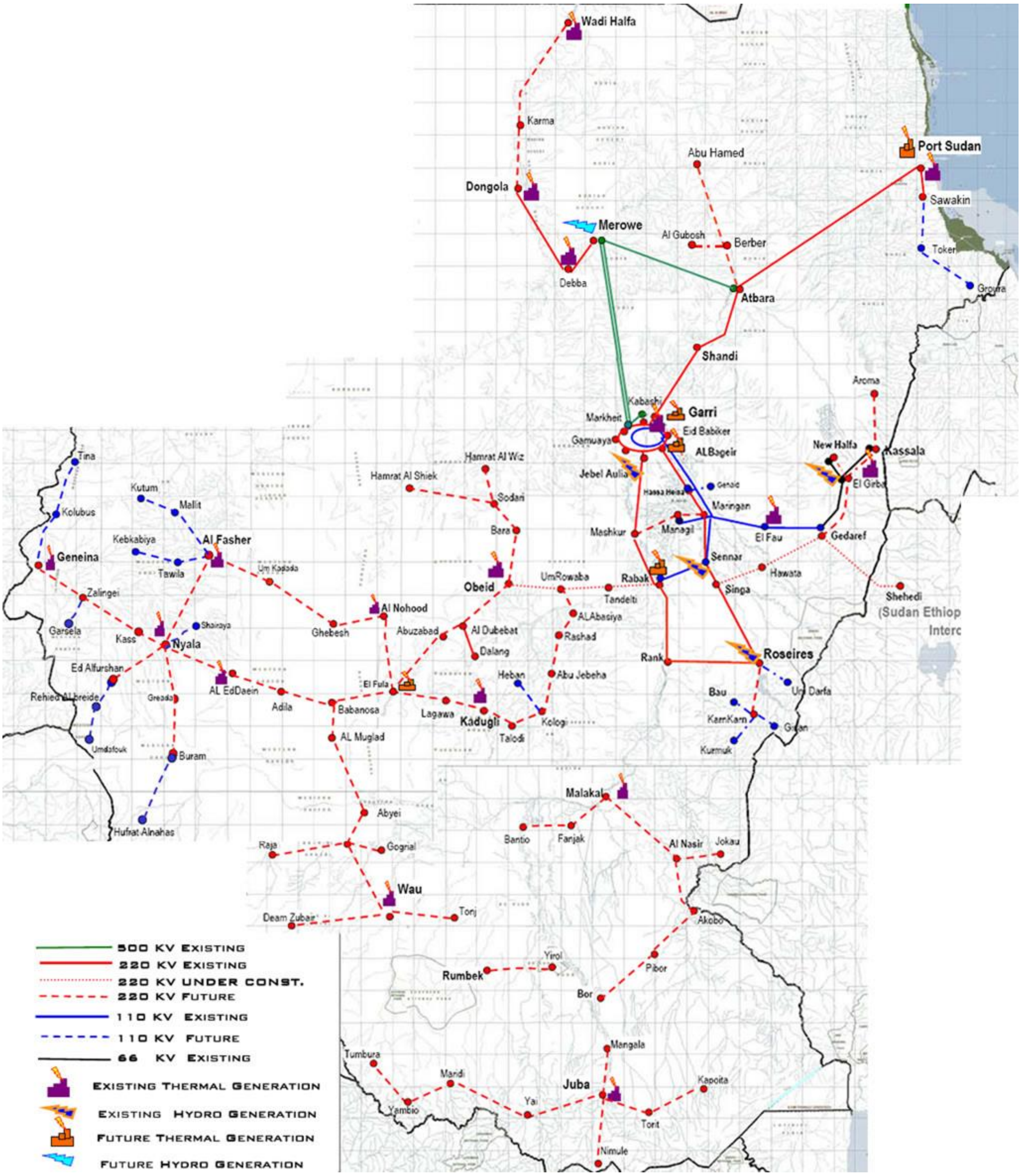

Figure 1. The Sudan National Power Grid map

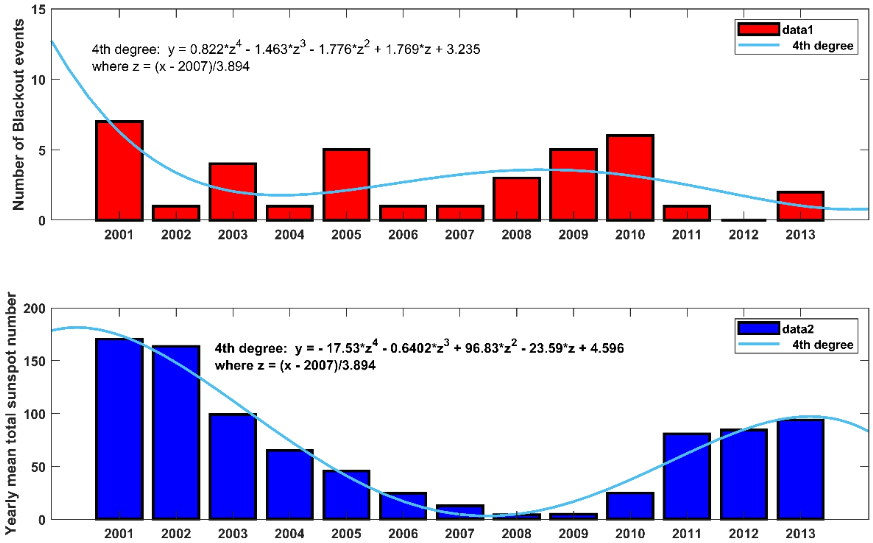

Figure 2. Upper panel shows occurrence of blackout events in the NPGS in years from 2001 to 2013, while the lower panel shows yearly mean total sunspot numbers for years from 2001 to 2013, and the 4th degree polynomial fit is shown for both data on the two panels.

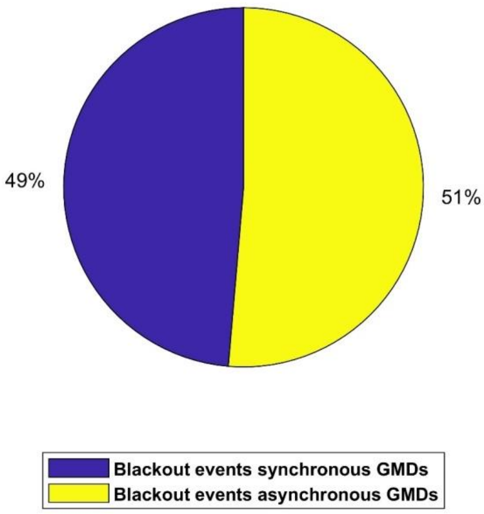

Figure 3. Blackout events in the NPGS in the period: 2001 to 2013 characterized in terms of blackout events synchronous geospace GMDs, and blackout events asynchronous GMDs.

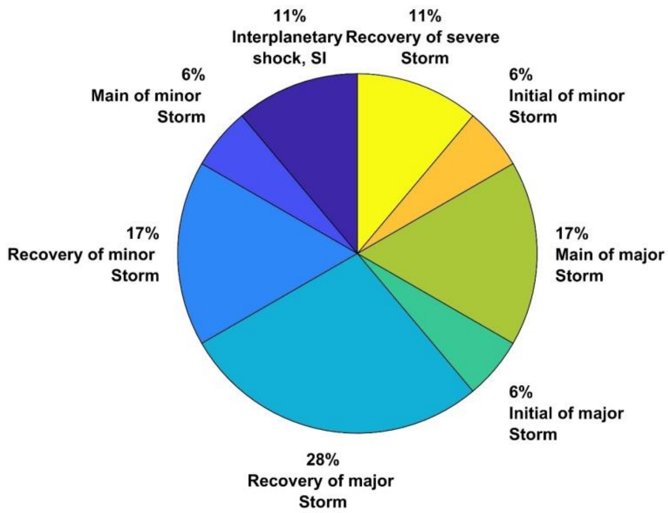

Figure 4. Blackout events synchronous storms, characterized for all storm classes.

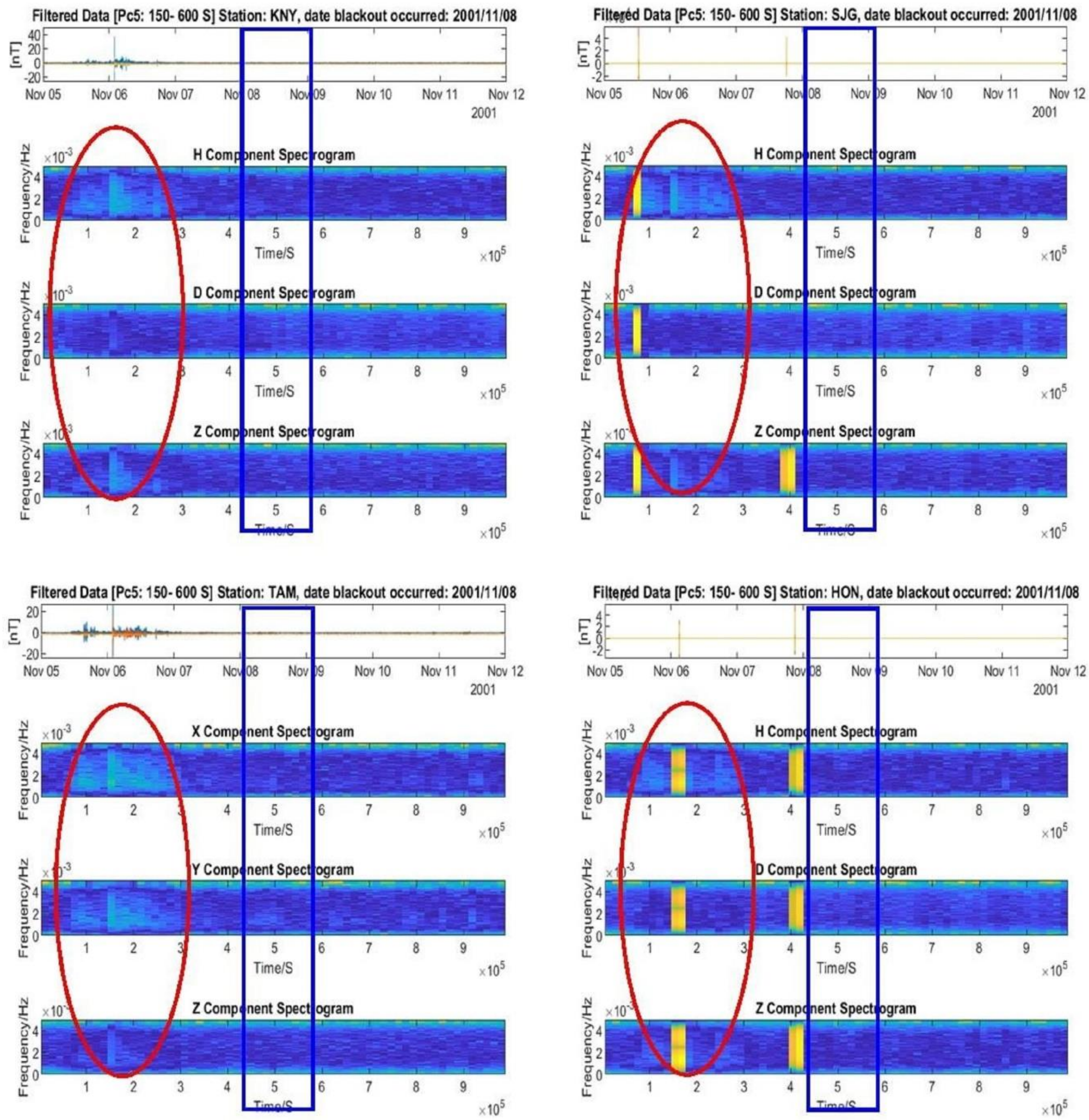

Figure 5. Shows magnetograms from INTERMAGNET stations (KNY, SJG, TAM, and HON). Top panel: filtered data in the period range: 150 – 600 s for the three components of the geomagnetic field, the two horizontal components (blue and red), and the vertical component (orange). Bottom panels (three): spectrogram of the same three components from upper to lower, respectively. The blue rectangle shows the day occurrence of the blackout event (08112001) synchronous a severe storm, while the red oval shape shows the enhanced amplitudes of the Pc5 pulsations.

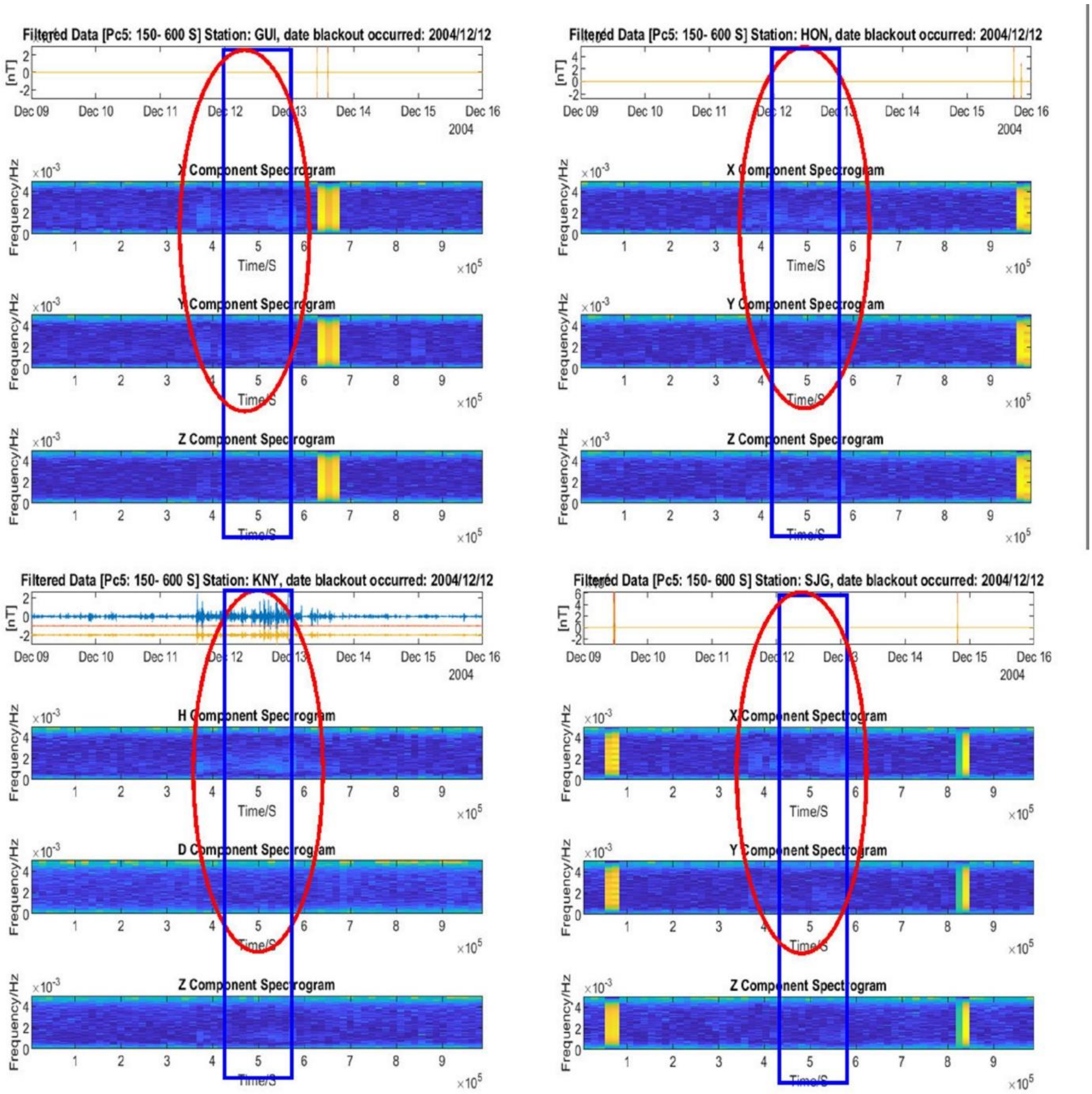

Figure 6. Shows magnetograms from INTERMAGNET stations (GUI, HON, KNY, and SJG). Top panel: filtered data in the period range: 150 – 600 s for the three components of the geomagnetic field, the two horizontal components (blue and red), and the vertical component (orange). Bottom panels (three): spectrogram of the same three components from upper to lower, respectively. The blue rectangle shows the day occurrence of the blackout event (12122004) synchronous a major storm, while the red oval shape shows the enhanced amplitudes of the Pc5 pulsations.

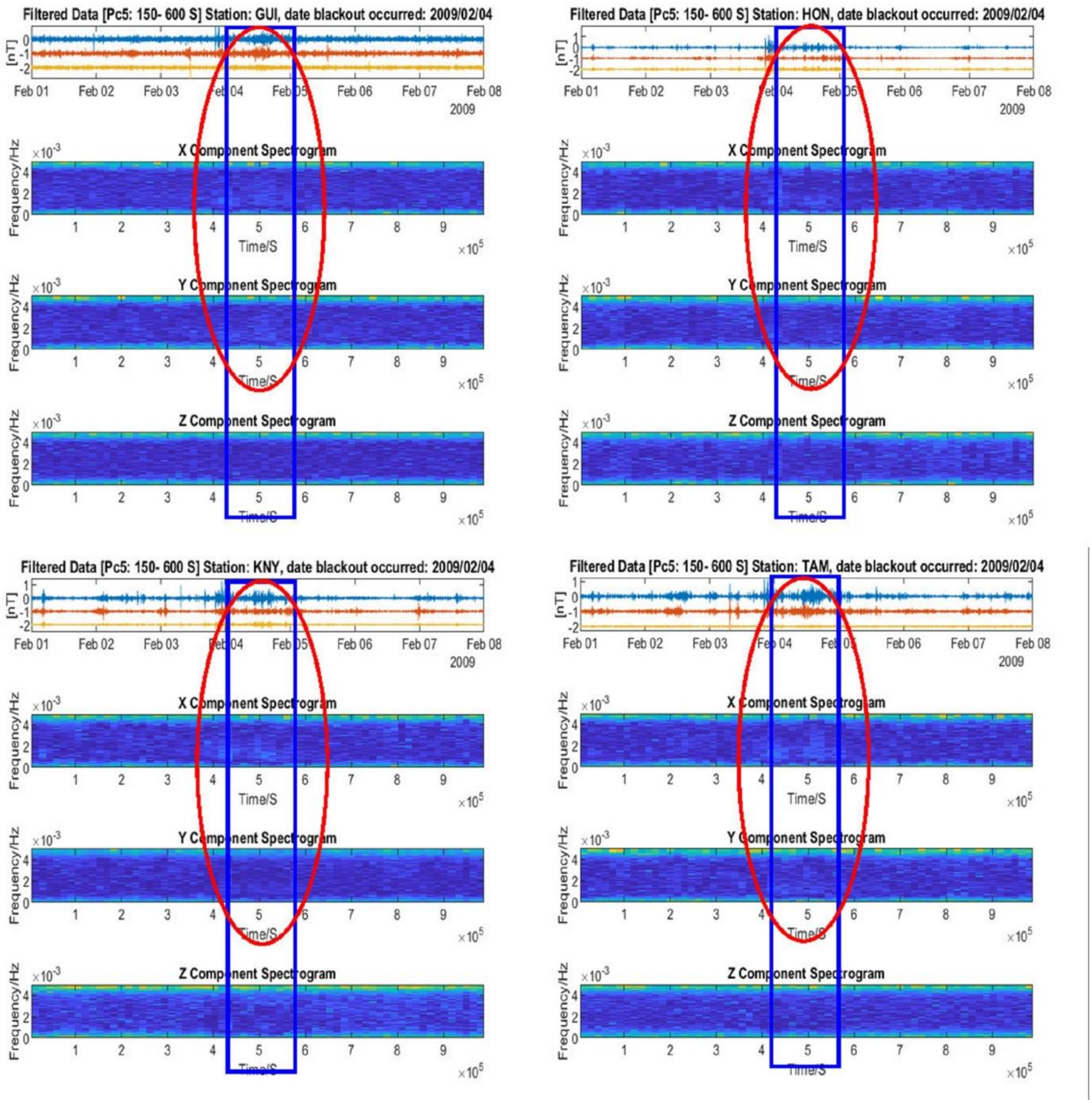

Figure 7. Shows magnetograms from INTERMAGNET stations (GUI, HON, KNY, and TAM). Top panel: filtered data in the period range: 150 – 600 s for the three components of the geomagnetic field, the two horizontal components (blue and red), and the vertical component (orange). Bottom panels (three): spectrogram of the same three components from upper to lower, respectively. The blue rectangle shows the day occurrence of the blackout event (04022009) synchronous a minor storm, while the red oval shape shows the enhanced amplitudes of the Pc5 pulsations.

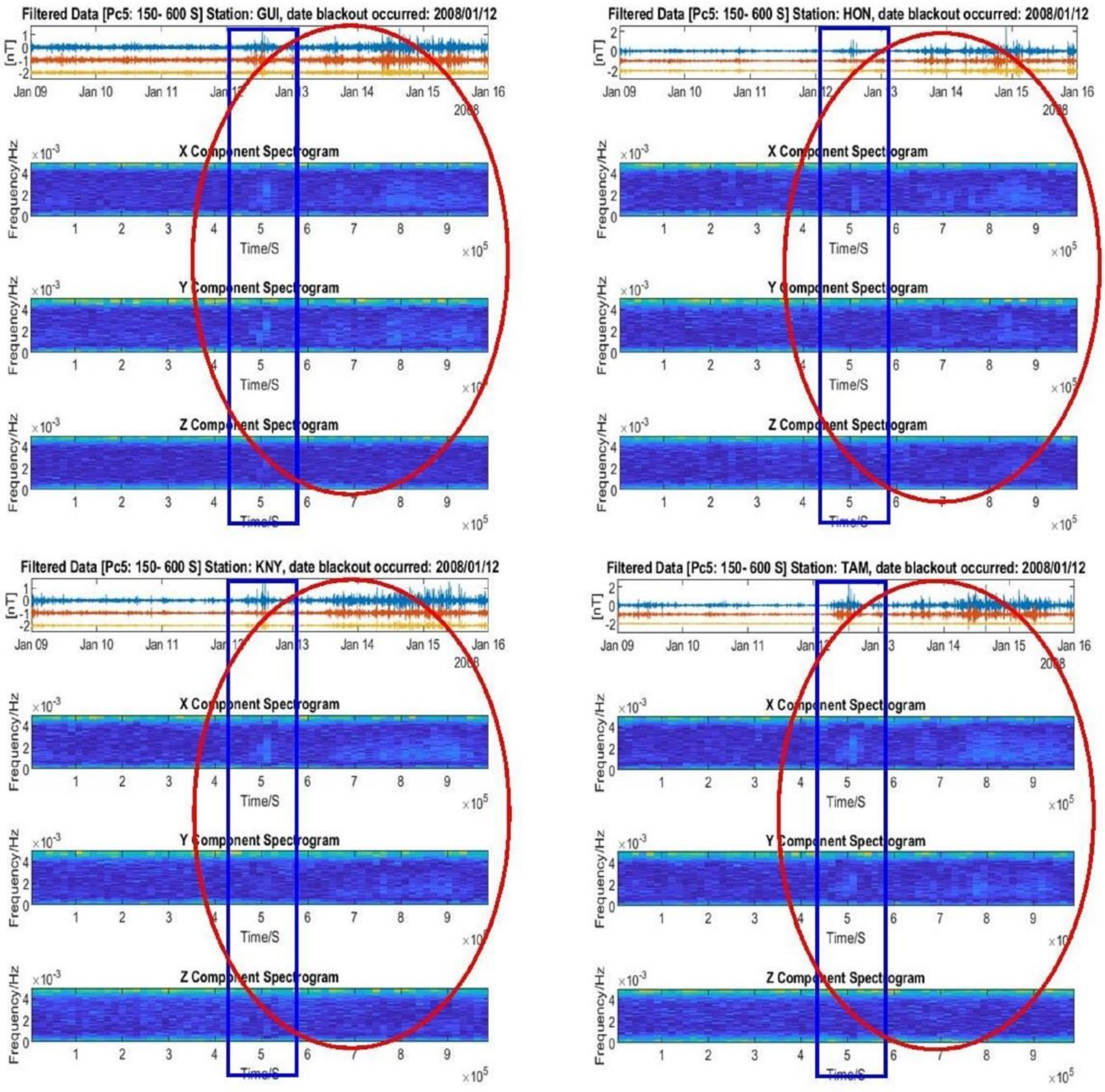

Figure 8. Shows magnetograms from INTERMAGNET stations (GUI, HON, KNY, and TAM). Top panel: filtered data in the period range: 150 – 600 s for the three components of the geomagnetic field, the two horizontal components (blue and red), and the vertical component (orange). Bottom panels (three): spectrogram of the same three components from upper to lower, respectively. The blue rectangle shows the day occurrence of the blackout event (12012008) synchronous a sudden impulse, SI, while the red oval shape shows the enhanced amplitudes of the Pc5 pulsations.